EDGE ARTICLE

Check for updates

Acoustic cavitation generates molecular mercury(II) hydroxide, Hg(OH)₂, from biphasic water/mercury mixtures†

Minjun Yang, [ID] Bertold Rasche [ID] and Richard G. Compton [ID] *

Emulsification of elemental mercury in aqueous solution in the form of grey particles occurs upon exposure to intense sound fields. We show the concomitant formation of molecular $Hg(OH)_2$ in the solution phase reaching a saturation limit of 0.24 mM at 25 °C. The formation of $Hg(OH)_2$ is consistent with the 'hot spot' model which suggests the formation of $OH^{\bullet}$ as a result of acoustic cavitation; such radicals are proposed to combine with Hg to form the $Hg(OH)_2$ species here characterised using voltammetry.

Introduction

'Acoustic cavitation', the formation and collapse of bubbles suspended in a liquid can occur on exposure to intense sound fields with frequencies ranging from audible sound to ultrasound.[1–3] When the bubbles collapse during the cavitation cycle photons are emitted with energies approximately eleven orders of magnitude higher as compared to the energy density of the sound field;[4] this phenomenon, known as sonoluminescence, sparked interest throughout scientific community with over 1000 papers published between 1990 to 2005.[5] The bubbles collapse near adiabatically, generating a 'hot spot' in which the temperature can reach 1000–10 000 K with a pressure >10^7 N m^{-2}.[5–8] Under these extreme conditions water molecules pyrolytically cleave to $H^{\bullet}$ and $OH^{\bullet}$.[9–11]

Separate studies report $OH^{\bullet}$ radicals, generated *via* photolysis of nitrate or methyl nitrite, can react with atomic mercury in both gaseous[12] and aqueous[13] phases as inferred indirectly from kinetic data with the possible formation of $HgOH^{\bullet}$ and/or $Hg(OH)_2$ suggested. Direct spectroscopic or other evidence for $Hg(OH)_2$ is sparse; an infra-red spectrum of $Hg(OH)_2$ deposited on solid neon and argon at 5 K has been reported[14] and is thought might play a role in the transport of inorganic mercury through lipid bilayer membranes.[15,16]

Metallic mercury at room temperature is immiscible with water. However, within tens of seconds of exposure to ultrasound sonication, a grey 'cloud' of particles is seen emanating from the mercury–water interface into the aqueous phase.[17–20] The particles in the resulting mercury emulsion sediment

within hours but do not re-merge with the bulk metallic mercury. Herein, we investigate the redox behaviour of the insonated mercury–water system, so as to generate $OH^{\bullet}$ *via* acoustic cavitation, and the possibility of $Hg(OH)_2$ formation. In particular electrochemical methods evidence $Hg(OH)_2$ in the solution phase which gives a voltammetric signature distinct from Hg^{2+} or Hg_2^{2+}.

Experimental

Chemicals

All chemicals used were of analytical grade and were purchased from Sigma-Aldrich (U.K) with the exception of metallic mercury purchased from Elgar Phosphors & Chemicals Ltd (U.K). All chemicals were used without further purification. Aqueous solutions were made using ultrapure water (Millipore, resistivity of 18.2 MΩ cm at 25 °C). The saturated solution of $Hg(OH)_2(aq)$ at 0.24 mM was made by stirring solution containing the equivalent amounts of HgO(s) in 0.1 M KNO_3 at an elevated temperature of 70 °C for 2 hours.[21]

Electrochemical cell

The electrochemical cell consists of three electrodes; a carbon microdisc working electrode (diameter = 7 μm, IJ Cambria Scientific Ltd, UK), a saturated mercury sulphate reference electrode MSE (ALS, Japan) and a carbon rod counter electrode. The electrochemical experiments were conducted with a computer controlled potentiostat (Bio-Logic SP200, France). The working electrode was cleaned after each experiment using alumina slurries of decreasing particle sizes: 1.0, 0.3 and 0.05 μm (Buehler, LakeBluff, IL, USA). All electrochemical experiments were thermostated at 25 °C.

Department of Chemistry, Physical and Theoretical Chemistry Laboratory, University of Oxford, South Parks Road, Oxford OX1 3QZ, UK. E-mail: Richard.Compton@chem.ox.ac.uk

Mercury emulsion and supernatant separation

The ultra-sound sonication of 1 mL of metallic mercury in 100 mL of aqueous 0.1 M KNO_3 was conducted in a SW1H Clifton ultrasonic water bath (37 kHz, Nickel-Electro Ltd, UK). During sonication, a 'cloud' of grey particles is seen emanating from the mercury–water interface into the aqueous phase. The grey emulsion (termed a "mercury emulsion" in this article) was collected at sonication times of 5, 10, 15, 25, 40 and 60 minutes for electrochemical analysis. The grey particles were separated from the mercury emulsion *via* centrifugation (Eppendorf® Centrifuge 5702, Hamburg, Germany) at 4000 rpm for 5 minutes; the clear supernatant was then separated from the sedimented grey particles for further electrochemical analysis. An experimental scheme is provided in the ESI.†

Results and discussion

A 0.1 M KNO_3 aqueous solution containing metallic Mercury was sonicated for times of 5, 10, 15, 25, 40 and 60 minutes and the resulting mercury emulsion was collected. Fig. 1 shows the resulting cyclic voltammogram (CV) recorded with a carbon micro-disc electrode. The voltammograms were swept reductively from an initial potential of +0.5 V *vs.* MSE with reversal from −0.6 V. No faradaic current was observed for 5 minutes of sonication time although emulsification occurred within tens of seconds. After a sonication time of 10 minutes or longer, a quasi-steady state cathodic current with a half-wave potential around −0.26 V *vs.* MSE can be seen, and approaches −0.9 nA after prolonged sonication times. The steady state cathodic current signals reduction of a solution phase species. During the reverse sweep, a near-symmetric "stripping" peak is observed at +0.05 V *vs.* MSE and the peak height evolves over 60 minutes of sonication time. Furthermore, at higher oxidative over-potentials 'spike-like' voltammetric behaviour sporadically occurs. Those oxidative signals, the stripping peak and the
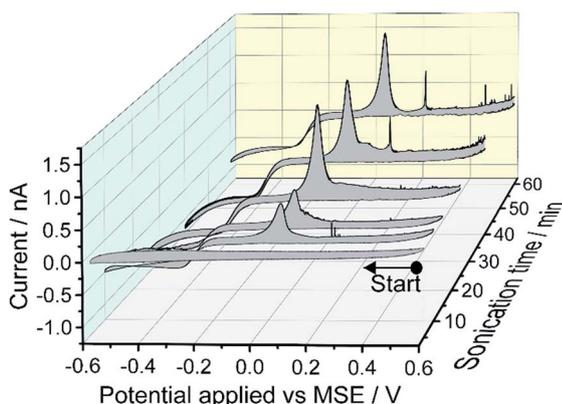
'spikes-like' events, are only seen during the reverse sweep suggesting oxidation of reduction product(s).

Next, a series of double-step chronoamperometry experiments were conducted; first, the potential was stepped to a negative potential of either −0.8, −0.4, −0.2, or 0.0 V *vs.* MSE for 30 s followed by a second potential step to a oxidative potential of +0.5 V for another 30 s. Fig. 2 plots the current–time transient recorded during the second potential step. As can be seen, both the magnitude and frequency of the oxidative 'spikes' increases with the magnitude of the applied negative over-potential (see ESI† for spike analysis). Note the electrode was polished in between experiments to produce a fresh surface.

In a next step, the emulsion particles were successfully separated from the mercury emulsion *via* centrifugation and both the supernatant and the particles were collected for analysis. The particles were characterised by X-ray diffraction showing broad peaks consistent with liquid mercury[22–24] and amorphous $HgO_{(am)}$, see ESI Section 2.† The amorphous $HgO_{(am)}$ is likely present as shells surrounding Hg droplets resulting in the matt grey, non-metallic particle appearance. To the best of our knowledge this is the first XRD study of an Hg emulsion and the first to show that it consists of Hg and amorphous $HgO_{(am)}$.

Fig. 3 shows the cyclic voltammograms of the supernatant solutions separated from the mercury emulsions prepared with different exposure times to sonication. Similar to the case of the mercury emulsion, presented in Fig. 1, a quasi-steady state cathodic current is seen and with a magnitude approaches to −0.8 nA; a subsequent oxidation peak can again be seen at +0.05 V. Thus, this evidences a soluble mercury(I) or mercury(II) complex present in the solution phase after tens of minutes of sonication and this is independent of the presence of the grey
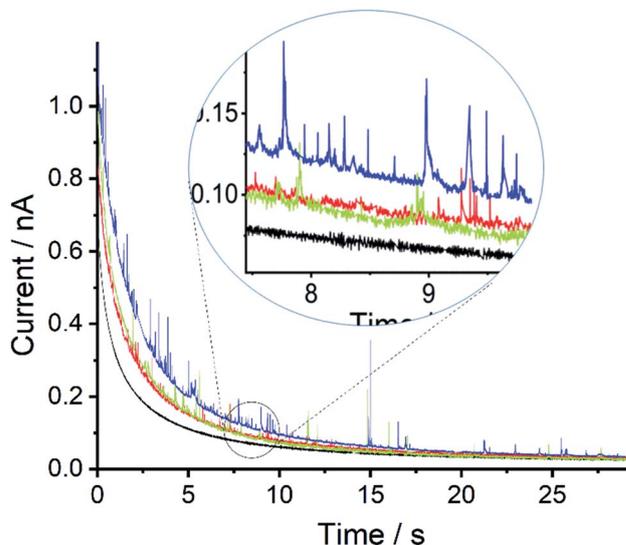

Fig. 1 Cyclic voltammograms of the grey mercury emulsions generated by ultra-sound sonication of an aqueous solution containing 0.1 M KNO_3 and metallic mercury for 5, 10, 15, 25, 40 and 60 minutes. The voltammograms were recorded on a carbon micro-disk electrode (diameter = 7 μm) at a scan rate of 20 mV s^{-1}.

Fig. 2 Chronoamperogram of the mercury emulsion with sonication time of 60 minutes. The potential step was first stepped to −0.8 V (blue), −0.4 V (green), −0.2 V (red) or 0.0 V (black) for 30 s then immediately to +0.5 V for 30 s. Note the graph shows the current–time transient during the second potential step.
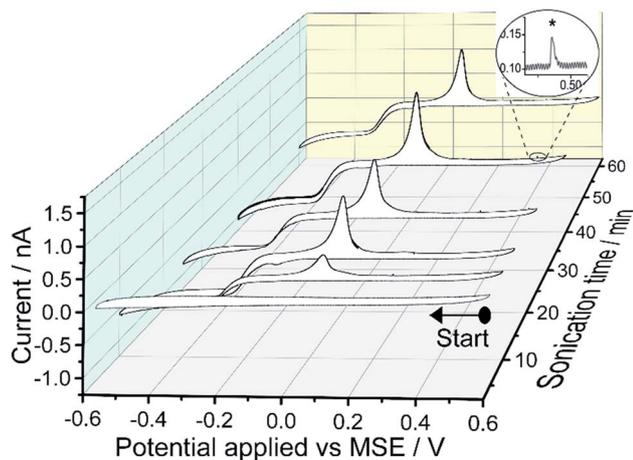
Fig. 3 Cyclic voltammograms of the supernatant separated from the mercury emulsion after sonication. The supernatant solution was obtained by centrifuging mercury emulsions at 4000 rpm for 5 minutes. The voltammetric experimental conditions are the same as Fig. 1. Inlay shows an examples of a small spikes (*).

particles which result from emulsification. The near symmetric oxidation peak at +0.05 V is attributed to the oxidation of Hg^0 at the electrode surface. Small oxidative spikes are seen and occur less frequently compared to the CV obtained in the mercury emulsion (Fig. 1).

Fig. 4 shows the voltammograms of a 'transfer' experiment where a reductive sweep (black line) was first conducted in the supernatant. The electrode was then rinsed with deionised water and subsequent transferred to a 0.1 M KNO_3 only electrolyte solution for "oxidative stripping" (red line). Both the stripping peak (E_{peak} at +0.05 V vs. MSE) and the 'spike' events
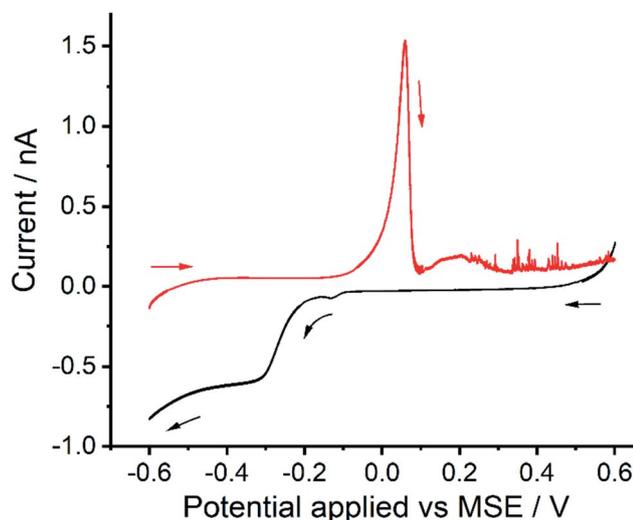

Fig. 4 Transfer experiment conducted with the supernatant separated from a mercury emulsion after 60 minutes of sonication. Black line shows the reductive linear sweep voltammetry (LSV) recorded in the supernatant. Subsequently, the electrode was rinse with deionised water and transferred to solution of 0.1 M KNO_3 for oxidative sweep, shown as red line. Scan rate was 20 mV s^{-1}.

are seen, suggesting both of the oxidation processes resulted from surface bound reduction products.

The physical origin of the spikes can be deduced from the above observations. First, the presence of mercury particles (Hg@HgO core–shell) in solution do not lead to direct oxidative spikes unless a negative over-potential is first applied (Fig. 2). Second, spikes are seen during the re-oxidation sweep in 0.1 M KNO_3 electrolyte (transfer experiment, Fig. 4). Thus, the 'spike-like' events are likely due to incomplete oxidation of surface-bound bulk mercury, resulting from the loss of small mercury droplets either into the solution phase, and/or as remnants on the electrode surface. These lead to sporadically occurring oxidation spikes as the droplets re-encounter the electrode or newly make electrical contact. As such these spikes are different in some respects to those seen in 'Faradaic impact electrochemistry' notably where nanomaterials are electrolysed.[25,26] Furthermore, the size and frequency of the occurring spikes in CVs recorded in the Hg@HgO core–shell particles containing emulsion solutions (Fig. 1) are higher than that seen in the supernatant solutions (Fig. 3), obtained under the same voltammetric conditions. A likely explanation is that the thin amphorous HgO shell layers surrounding the Hg@HgO core–shell particles are reduced during the cyclic voltammetry, contributing their reservoir of core mercury to form more surface-bound mercury at the electrode surface.

It is evident that, a mercury(I) or mercury(II) complex soluble in the solution phase, after exposure to ultrasound, is electrochemically visible. The identity of this species is next considered. Plausible sono-chemical reactions include first hydroxyl radicals OH$^{\bullet}$ – formed via cavitation – reacting directly with Hg^0 to form soluble $Hg(OH)_2$(aq) via eqn (1)–(3)

$$Hg^0 + OH^{\bullet} \rightarrow HgOH^{\bullet} \tag{1}$$

$$HgOH^{\bullet} + OH^{\bullet} \rightarrow Hg(OH)_2 \tag{2}$$

$$HgOH^{\bullet} + O_2 + H_2O \rightarrow Hg(OH)_2 + H^+ + O_2^- \tag{3}$$

and/or second, oxidation of elemental mercury Hg^0, via electron transfer, by radical derived oxidants [Ox] to form Hg_2^{2+}(aq) or Hg^{2+}(aq) ions

$$Hg \xrightarrow{[Ox]} \frac{1}{2}Hg_2^{2+} \xrightarrow{[Ox]} Hg^{2+} \tag{4}$$
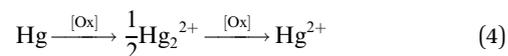
where Ox might be OH$^{\bullet}$, H_2O_2 or HOO$^{\bullet}$ etc. Accordingly, we next compare and contrast the redox behaviour of the supernatant with solutions containing different mercury(I) or mercury(II) complexes. A solution of $Hg(OH)_2$ is thought to be obtained by dissolution of solid mercury(II) oxide

$$HgO(s) + H_2O(l) \rightleftharpoons Hg(OH)_2(aq) \tag{5}$$

The limit of dissolution of solid HgO in water at 298 K is 0.052 g dm^{-3} which corresponds to a saturation limit of 0.24 mM $Hg(OH)_2$.[21] $Hg(OH)_2$(aq) is known not to dissociate to Hg^{2+} and OH$^-$.[27]

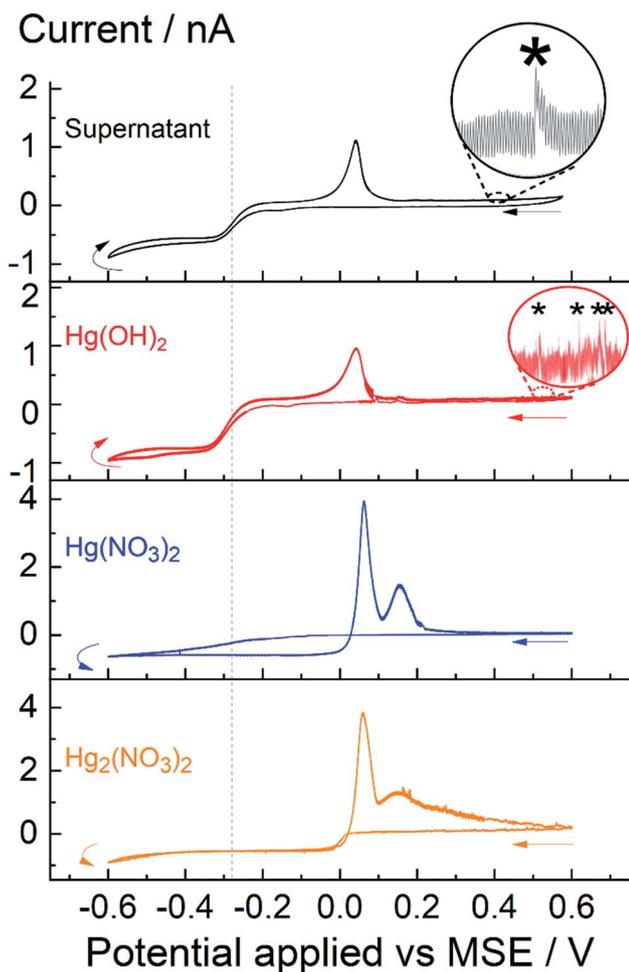Fig. 5 shows four cyclic voltammograms obtained with the supernatant and three other mercury species; overlaid in the

Current / nA

Fig. 5 Cyclic voltammograms various mercury(ɪ) or mercury(ɪɪ) ion containing 0.1 M KNO₃ solutions. Black line – supernatant obtained after 60 minutes of sonication; red line –saturated solution of Hg(OH)₂(aq) obtained *via* dissolution of 0.24 mM HgO; blue line – 0.24 mM Hg(NO₃)₂; orange line – 0.24 mM Hg₂(NO₃)₂. The grey dotted line indicates the half-wave potential at −0.28 V. Inlay shows examples of small spikes (*).

top-half are: supernatant obtain after 60 minutes of sonication, saturated concentration of 0.24 mM Hg(OH)₂ obtained *via* dissolution of HgO; overlaid in the bottom-half are 0.24 mM of Hg₂(NO₃)₂ and Hg(NO₃)₂. In all cases, the potential was swept reductively from +0.6 V to −0.6 V *vs.* MSE. For the supernatant solution, obtained after 60 minutes of insonation, a quasi-steady state cathodic current is seen approaching to −0.8 nA as mentioned above. Similarly, the steady state cathodic current for the saturated solution of Hg(OH)₂, obtained by dissolution of HgO, approaches to −0.9 nA with a half-wave reduction potential seen around −0.28 V *vs.* MSE (indicated by the grey dotted line). In comparison, the voltammometric signal for Hg_2^{2+}(aq) and Hg^{2+}(aq) – at equal concentration of 0.24 mM – are distinctively different to that seen for Hg(OH)₂; first, the cathodic steady state current approaches to −0.6 nA and second, a hysteresis/cross-over in current are seen in the voltammograms of Hg_2^{2+} and Hg^{2+}. It is likely that deposition of

mercury on a carbon surface changes both the electrode kinetic and surface morphology during the voltammetric sweep and thus leading to the reduction of Hg_2^{2+} and Hg^{2+} ions at higher oxidation potential on the reverse sweep. Similar behaviour was seen on a Pt electrode (see ESI†).

It is evident that, insonation of a mercury–water system generates soluble Hg(OH)₂ which is visible voltammetrically. The electrode kinetics of Hg(OH)₂ is irreversible with a cathodic transfer coefficient around 0.5. Moreover, the magnitude of the steady state current I_{ss} recorded on a micro-disk electrode is directly proportional to the concentration (C) and diffusion coefficient (D) of the analyte

$$I_{ss} = 4nFDCr \tag{6}$$

where n is the number of electrons transferred, F is the Faraday constant and r is radius of the micro-disc electrode. Thus, a diffusion coefficient of Hg(OH)₂, 1.4×10^{-9} m² s⁻¹, in aqueous solution at 298 K can be deduced from the saturated Hg(OH)₂ solution, obtained *via* dissolution of HgO, with a known concentration of 0.24 mM.

Conclusions

Insonation of mercury/water system leads to grey emulsions in which the particles have been characterised as Hg@HgO core–shell structures. Further, a molecular mercury species in the solution phase – after insonation of mercury–water system – is voltammetrically visible and characterised as that of Hg(OH)₂, a possible intermediate in the sonochemical formation of HgO. The voltammetric signatures of Hg(OH)₂ are distinctively different to the freely solvated Hg_2^{2+} and Hg^{2+} ions, with noticeably different half-wave potentials and an absence of hysteresis in the current during the reverse sweep. The formation of molecular Hg(OH)₂ is consistent with the 'hot spot' model in which generation of OH˙ *via* cavitation leading to concomitant reactions with elemental mercury to form Hg(OH)₂. Moreover, the cathodic steady state current of −0.8 nA recorded with the supernatant, obtained after 60 minutes of insonation, suggest a concentration approaching the saturation limit of 0.24 mM at 298 K.

Conflicts of interest

There are no conflicts to declare.

Acknowledgements

Notes and references

1 L. A. Crum, T. J. Mason, J. L. Reisse and K. S. Suslick, *Sonochemistry and sonoluminescence*, Springer Science & Business Media, 2013.

2 K. S. Suslick, *Ultrasound: its Chemical, Physical, and Biological effects*, VCH Publishers, 1988.

3 G. J. Price, *Current Trends in Sonochemistry*, Royal Society of Chemistry, 1992.

4 B. P. Barber and S. J. Putterman, *Nature*, 1991, **352**, 318.

5 L. A. Crum, *J. Acoust. Soc. Am.*, 2015, **138**, 2181–2205.

6 W. B. McNamara III, Y. T. Didenko and K. S. Suslick, *Nature*, 1999, **401**, 772.

7 E. B. Flint and K. S. Suslick, *Science*, 1991, **253**, 1397–1399.

8 P. Jarman, *J. Acoust. Soc. Am.*, 1960, **32**, 1459–1462.

9 G. J. Price, M. Ashokkumar, M. Hodnett, B. Zequiri and F. Grieser, *J. Phys. Chem. B*, 2005, **109**, 17799–17801.

10 R. Pflieger, H. P. Brau and S. I. Nikitenko, *Chem.–Eur. J.*, 2010, **16**, 11801–11803.

11 K. S. Suslick, S. J. Doktycz and E. B. Flint, *Ultrasonics*, 1990, **28**, 280–290.

12 J. Sommar, K. Gårdfeldt, D. Strömberg and X. Feng, *Atmos. Environ.*, 2001, **35**, 3049–3054.

13 K. Gårdfeldt, J. Sommar, D. Strömberg and X. Feng, *Atmos. Environ.*, 2001, **35**, 3039–3047.

14 X. Wang and L. Andrews, *Inorg. Chem.*, 2005, **44**, 108–113.

15 J. Gutknecht, *J. Membr. Biol.*, 1981, **61**, 61–66.

16 T. Barkay, M. Gillman and R. R. Turner, *Appl. Environ. Microbiol.*, 1997, **63**, 4267–4271.

17 R. W. Wood and A. L. Loomis, *London, Edinburgh Dublin Philos. Mag. J. Sci.*, 1927, **4**, 417–436.

18 C. Bondy and K. Söllner, *Trans. Faraday Soc.*, 1935, **31**, 843–846.

19 E. C. Marboe and W. A. Weyl, *J. Appl. Phys.*, 1950, **21**, 937–938.

20 C. Bondy and K. Söllner, *Trans. Faraday Soc.*, 1936, **32**, 556–567.

21 T. P. Dirkse, *Copper, Silver, Gold & Zinc, Cadmium, Mercury Oxides & Hydroxides*, Elsevier, 2016.

22 L. Bosio, R. Cortes and C. Segaud, *J. Chem. Phys.*, 1979, **71**, 3595–3600.

23 B. R. Orton and R. L. T. Street, *J. Phys. C: Solid State Phys.*, 1972, **5**, 2089.

24 V. G. Rivlin, R. M. Waghorne and G. I. Williams, *Philos. Mag.*, 1966, **13**, 1169–1179.

25 Z. Sofer, D. Bouša, J. Luxa, V. Mazanek and M. Pumera, *Chem. Commun.*, 2016, **52**, 1563–1566.

26 K. J. Stevenson and K. Tschulik, *Curr. Opin. Electrochem.*, 2017, **6**, 38–45.

27 A. B. Garrett and A. E. Hirschler, *J. Am. Chem. Soc.*, 1938, **60**, 299–306.